

CHAPTER 215

Vertically Varying Velocity Field in Q-3D Nearshore Circulation

A. Sánchez-Arcilla, F. Collado and A. Rodríguez¹

Abstract

This paper presents an efficient and economic technique to obtain vertical profiles for surf-zone wave-induced currents. The current-wave bottom boundary layer is solved in a parameterized manner, while employing a power series approximation to obtain the solution in the middle layer (extending up to trough level). This "profile extraction technic" has been coupled to a 2DH surf-zone circulation model which is also concisely described. The paper ends with a brief discussion of some obtained results part of the calibration work which is a very much on going task.

1. Introduction

This paper presents a solution for the vertically varying velocity field in a Q-3D modelling context. It is part of an improved version of the Quasi- 3D NEARCIR Model (S.-Arcilla et al., 1990/91) developed during the MAST-I G6M (Currents) Project. The proposed model is able to achieve a detailed simulation of nearshore flows at a reasonable cost (cheaper than a full 3D code). The model works at the current time scale and it is structured into three modules (see fig. 1):

- i) Wave Propagation Module.
- ii) Depth Uniform Current Module.
- iii) Depth Varying Current Module (including Bottom Boundary Layer).

¹ Lab. Ing. Marítima , L.I.M., Univ. Politécnic de Cataluña, U.P.C.
Av. Gran Capitán s/n, 08034 Barcelona, Spain.

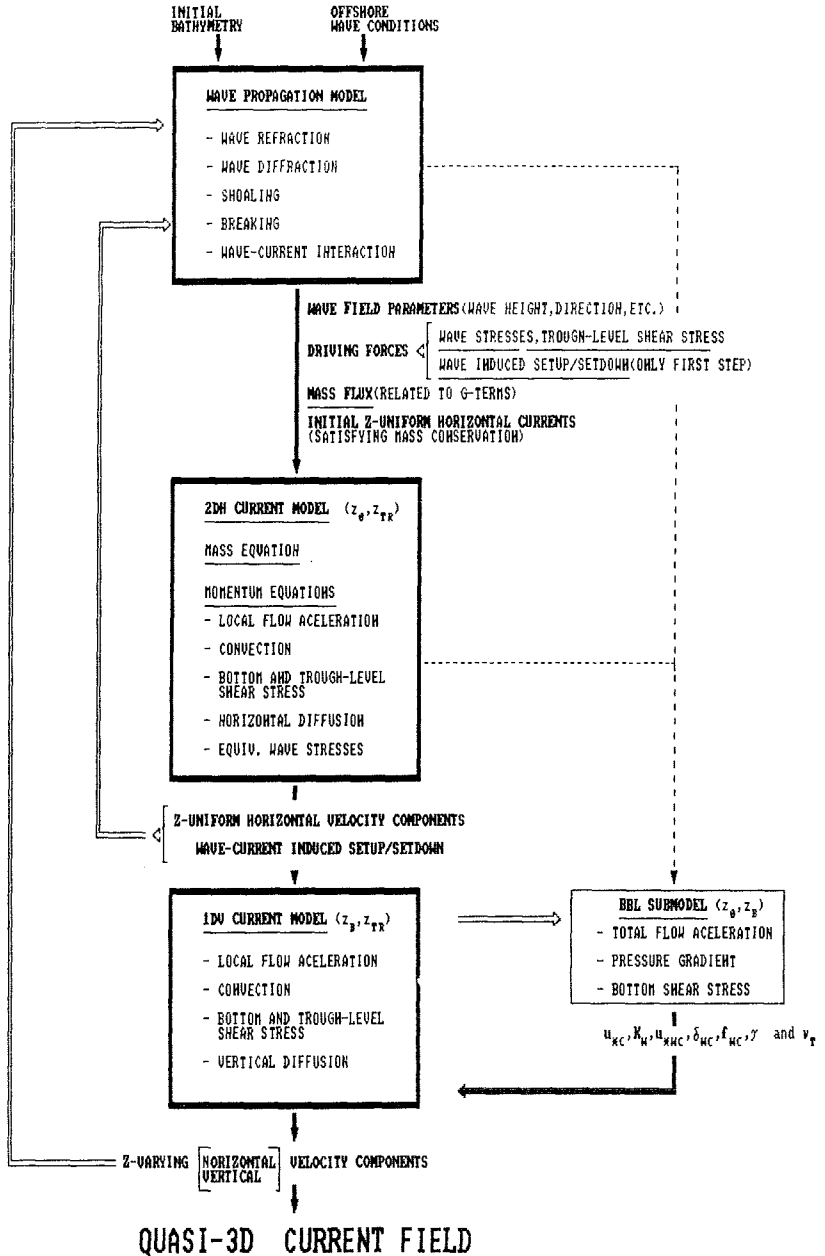


Fig. 1: NEARCIR flow chart.

The three modules operate in a sequential iterative manner (Wave—>Depth Uniform Current—>Depth Varying Current). Iterations are performed until certain prefixed convergence criteria are met. Each module is solved for a stationary solution before going on to the next one.

This paper will concentrate on the depth current module, the main new contribution being the coupling between middle and current-wave boundary layers.

2. Global Model

The model here presented considers a domain vertically splitted into three layers (figure 2). To achieve a Q-3D approach (2DH + 1DV) the total current velocity vector \vec{u} , is conveniently splitted into depth uniform, \vec{u} , and depth varying \vec{u} , components.

$$\vec{u} = \vec{u} + \vec{u} \quad , \quad (1)$$

where :

$$\int_{z_0}^{z_{tr}} \vec{u} dz = 0 \quad \text{and} \quad \int_{z_0}^{z_{tr}} \bar{v} \hat{u} dz = \bar{v} \int_{z_0}^{z_{tr}} \hat{u} dz = 0 \quad \forall \bar{v}, \hat{u} \quad (2)$$

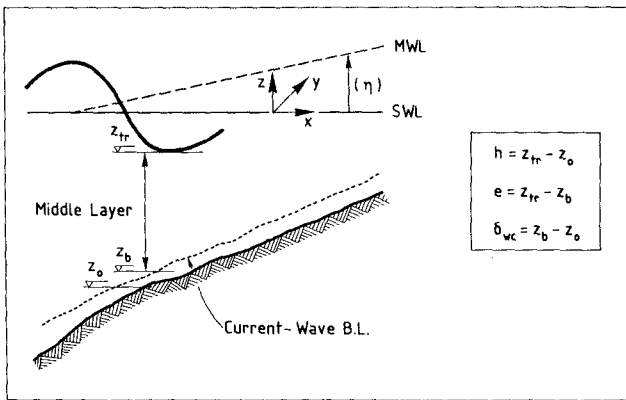


Fig. 2: Physical domain.

The upper layer is not solved. It is considered exclusively through its effects (interaction) with the middle layer via boundary conditions at trough level z_{tr} . These boundary conditions are related to the mass and momentum fluxes in the upper layer. The formulation obtained in this manner appears to be more consistent from a physical standpoint (identical boundary conditions for \bar{u} and \bar{u} , etc...) even though it also appears to be more sensitive to the selected closure submodels.

The depth-uniform Current Module solves a set of 2DH rigid-lid mass and momentum equations in a quite general manner. The equations and solution procedure have been presented elsewhere (S.-Arcilla et al. 1990). The wave driving terms appearing in these 2DH equations are:

$$\tilde{W}_i = -\frac{1}{\rho} \frac{\partial S_{ij}}{\partial x_j} - \langle \tilde{u}_i \tilde{u}_3 \rangle \Big|_{z_o}^{z_{tr}}$$

In expanded notation the x component (similarly for y) is:

$$\tilde{W}_x = -\frac{\partial}{\partial x} \int_{z_o}^{z_{tr}} \langle \tilde{u}^2 - \tilde{w}^2 \rangle dz - \frac{\partial}{\partial y} \int_{z_o}^{z_{tr}} \langle \tilde{u} \tilde{v} \rangle dz - \langle \tilde{u} \tilde{w} \rangle \Big|_{z_o}^{z_{tr}} \quad (3)$$

in which $\langle \rangle$ denotes time averaging at the scale of the waves and $(\tilde{u}, \tilde{v}, \tilde{w})$ is the wave velocity vector.

It is important to remark that this term is different from the classical radiation stress tensor due to the integration limits (actual bottom and trough level) and to the inclusion of (\tilde{u}, \tilde{w}) and (\tilde{v}, \tilde{w}) correlations.

The wave velocity field is given by the real part of the gradient of a velocity potential whose expression is:

$$\phi = Z(z) \epsilon(x, y) \exp(-i\omega t) \quad (4)$$

$$\epsilon(x, y) = \frac{-ig}{\sigma} A \exp(iS) \quad (5)$$

in which ω is the observed or apparent wave frequency. The wave-number vector $\vec{K} = (K_1, K_2)$ is given by $\vec{K} = \vec{\nabla}_H S$ and Z is the vertical shape function.

Assuming a horizontally varying amplitude field (due to breaking effects and/or diffraction caused by, for instance, a detached breakwater) and a doppler-shifted wave frequency due to the currents, the resulting wave velocity correlations obtained are (for illustration only the correlation product of vertical and horizontal velocities is here presented):

$$\langle \vec{u}_H \vec{w} \rangle = \frac{1}{2} \frac{g^2}{\sigma^2} \frac{\partial Z}{\partial z} Z A \vec{\nabla}_H A \tag{6}$$

in which σ is the intrinsic frequency. Equation (6) could also be considered a generalization for a 2DH context of the expression given by Deigaard and Fredsøe (1989) for normal incidence.

The resulting wave driving terms can then be written as:

$$S_{ij} = \frac{\rho}{2} \left[\left(\frac{1}{A^2} \frac{\partial A}{\partial x_i} \frac{\partial A}{\partial x_j} + K_i K_j \right) I_1(z_{tr}) + \delta_{ij} I_2(z_{tr}) \right] \frac{g^2}{\sigma^2} A^2 \tag{7}$$

with:

$$I_1(z) = \int_{z_o}^z Z^2 dz \quad ; \quad I_2(z) = \int_{z_o}^z \left(\frac{\partial Z}{\partial z} \right)^2 dz \tag{8}$$

A linear dispersion relation has been used to obtain σ in terms of k and with k satisfying a Battjes (1968) type relationship:

$$\vec{K} \cdot \vec{K} = k^2 + \frac{\Delta_H A}{A} \tag{9}$$

These expressions are similar to the classical equations for the radiation stress tensor when the upper limit of integration is equal to mean water level and the correlations of horizontal/vertical wave velocities are taken as 0 (Dingemans et al. 1987). For a more complete derivation where current variations have been considered see Rivero and S.-Arcilla (1992).

The three remaining unknowns are the wave amplitude A and the wave number vector \vec{K} , which are obtained by means of a coupled system of equations: the wave action balance equation and the kinematic conservation principle (Yoo and O'Connor 1986/88).

3. Depth-varying current module

An alternative treatment to solve coupledly the middle and bottom-boundary layers is here proposed. The Bottom Boundary Layer Model, strongly inspired on Fredsøe (1984), has been parameterized to be compatible with the quasi-3D cost/efficiency philosophy.

3.1 Middle layer

The momentum equations in the middle layer are obtained by subtracting the depth-integrated equations from the general ones. Only a simplified version of these momentum equations for \vec{u} is presented here:

$$\frac{\partial \vec{u}}{\partial t} + A\vec{u} - \frac{\partial}{\partial z}(\nu_V \frac{\partial \vec{u}}{\partial z}) = \vec{T}(z) \quad (10)$$

With

$$\vec{T}(z) = \frac{\langle \vec{\tau}_o \rangle}{\rho e} - \frac{\langle \vec{\tau}_{tr} \rangle}{\rho e} - 2G\nabla G (P_W^2 - \bar{P}_W^2) \quad (11)$$

$$A = \begin{pmatrix} \frac{\partial \bar{u}}{\partial x} & \frac{\partial \bar{u}}{\partial y} \\ \frac{\partial \bar{v}}{\partial x} & \frac{\partial \bar{v}}{\partial y} \end{pmatrix} \quad (12)$$

$$G = \nabla_H \langle \vec{Q}_s \rangle \quad (13)$$

with \vec{Q}_s being the wave plus current volume flux in the crest-to-trough layer and P_W the vertical distribution function of the vertical current velocity, W . The thickness of the middle layer is given by e and $\langle \vec{\tau}_{tr} \rangle$ and $\langle \vec{\tau}_o \rangle$ are, respectively, the shear stresses at trough and bottom levels.

The main hypotheses required to derive this simplified version of the momentum equation are: i) linearization (in \vec{u}) of convective terms, ii) neglect horizontal gradients of \vec{u} , iii) neglect Coriolis effects and iv) neglect vertical nonuniformities of wave stresses. This is the equation that has been applied in the middle layer (z_b, z_{tr}).

3.2 Bottom boundary layer

The model selected for this (z_o, z_b) layer is similar to the one proposed by Fredsøe in 1984. It was selected based on a comparison of its numerical results with data and other numerical model results (Simons et al. 1988) and

an extensive intercomparison exercise performed during MAST-I. This model does not consider turbulence from the previous wave and assumes logarithmic velocity profiles for both waves and currents. Two matching boundary conditions are applied at the top of the boundary layer, $z_b = \delta_m + K_N/30$, viz. continuity of current velocity and shear-stress (in the current direction). The momentum equation perpendicular to the current velocity is used to obtain an expression of the instantaneous friction velocity, u_* , as a function of the wave phase. This equation is solved using a classic Runge-Kutta method of sixth order.

3.3 Boundary conditions between middle layer and bottom boundary layer

At the top of the current-wave boundary layer, z_b , the present approach assumes: i) continuity of current velocity u , ii) continuity of $\langle \tau \rangle$ (in the current plane), iii) discontinuities of u_* (from now on shear-stress at the current time-scale), $\frac{\partial \vec{u}}{\partial z}$, and $\nu_V(z_b)$. For illustration, the current shear velocity jumps from u_{*wc} (below z_b) to u_{*c} (above z_b). The corresponding $\frac{\partial \vec{u}}{\partial z}$ values are:

$$\left. \frac{\partial \vec{u}}{\partial z} \right|_{z_b}^- = \frac{u_{*wc}}{(\delta_m + K_N/30)\kappa} \tag{14}$$

$$\left. \frac{\partial \vec{u}}{\partial z} \right|_{z_b}^+ = \frac{u_{*c}^2}{\nu_V(z_b)} \tag{15}$$

in which δ_m is the mean boundary layer thickness and κ von Karman's constant.

The values of \vec{u} and $d\vec{u}/dz$ at the top of the bottom boundary layer (BBL) provided by this model are used as boundary conditions for the middle layer (ML) equations. The third boundary condition is $d\vec{u}/dz$ at z_{tr} , obtained through the ν_V and $\langle \vec{\tau}_{tr} \rangle$ closure submodels. The apparent excess of a boundary condition (over stated problem) is solved by considering that the friction (wave plus current) velocity at the top of the BBL is still unknown. u_{*c} at z_b^+ is in fact due to bottom-induced turbulence but should also be affected by breaking-induced turbulence. This u_{*c} can be mathematically considered as an extra degree of freedom to obtain a well defined problem that is solved using an iterative process between ML and BBL.

4. Numerical solution of Depth Varying Current Module

4.1 Numerical solution of \vec{u} equations

The middle layer equations are solved using a power series approximation ($a_i z^i$) to reproduce the vertical variation of the unknown \vec{u} and the right-hand-side term of the equation. Time is used as a marching variable since only

stationary currents are here considered (to be consistent with the rigid lid approximation of the 2DH equations). The semi-discrete version of equation (10) can be arranged to yield at step $n+1$ (after discretization of the time derivative):

$$\underbrace{(I + \Delta t A)}_{A_t} \vec{u}^{\overline{n+1}} - \frac{\partial}{\partial z} \left(\Delta t \nu_V(z) \frac{\partial \vec{u}^{\overline{n+1}}}{\partial z} \right) = \underbrace{\vec{T}(z) \Delta t + \vec{u}^{\overline{n}}}_{\vec{R}(z)} \quad (16)$$

After a change of variable to simplify the vertical domain of variation to the interval $(0,1)$ and to uncouple the (\hat{u}, \hat{v}) equations, the following power series are introduced into the resulting momentum equation:

$$\left. \begin{aligned} \vec{w}(\xi) &= \sum_0^M \vec{w}_i \xi^i \\ \vec{R}(\xi) &= \sum_0^M \vec{r}_i \xi^i \\ K_t(\xi) &= K_0 + K_1 \xi + K_2 \xi^2 \end{aligned} \right\} \quad (17)$$

in which ξ is a normalized vertical coordinate, \vec{R} is the right hand side term of the equation and K_t is proportional to the eddy viscosity coefficient (for which a parabolic vertical distribution has been assumed). Using equations (16) and (17) a recurrence relation for the w_i coefficients for each component is obtained:

$$w_{i+1} = \left[-e^2 r_{i-1} + (\lambda e^2 - K_2 i(i-1) w_{i-1} - i^2 K_1 w_i) \right] \frac{1}{K_0(1+i)i} \quad (18)$$

$i = 1, \dots, M$

in which λ is the corresponding eigen-value coming from the uncoupling of the \hat{u} / \hat{v} equations.

The solution algorithm starts from $\frac{d\hat{u}}{dz}(z_b)$ and $\vec{\hat{u}}(z_b)$ values (given by the BBL model in terms of u_{*c} , u_{*wc} , δ_m and the artificial wave roughness K_w) until $\langle \vec{r}_{tr} \rangle$ is equal to the value given by the external closure submodel. Iterations are performed using u_{*c} as a degree of freedom until a convergence condition at z_{tr} is satisfied.

4.2 BBL Parameterization

The main BBL equation to be solved is the momentum equation perpendicular to \vec{u} , with gives $u_*(t)$ as a function of u_{*c} , U_m (wave orbital velocity), θ (wave phase) and γ (wave-current angle). From the obtained numerical solution the principal BBL variables (δ_m , K_w , u_{*wc} and u_{*c}) have been parameterized by means of "simple" algebraic expressions. For illustration purposes only the δ_m parameterization is shown here. $\frac{\delta_m}{K_N}$ is modeled by means of:

$$\frac{\delta_m}{K_N} = \frac{\delta_{90}}{K_N}(\varphi_c, \varphi_a, \gamma = 90^\circ) + \frac{\Delta\delta_\gamma}{K_N}(\varphi_c, \varphi_a, \gamma) \tag{19}$$

$$\varphi_c = \frac{u_m}{u_{*c}}, \varphi_a = \frac{a}{K_N}$$

in which a is the amplitude of the wave orbital motion and K_N is the Nikuradse roughness parameter. δ_{90} is the boundary layer thickness for waves perpendicular to the current and $\Delta\delta_\gamma$ is the deviation from the perpendicular case. The resulting δ_m is shown in figure 3. As it may be seen, $\frac{\delta_{90}}{K_N}$ can be modeled by linear expressions at both tails and by an exponential expression in the middle. The deviation, $\frac{\Delta\delta_\gamma}{K_N}$ is modeled by means of another exponential expression.

The maximum error (with respect to the original numerical results of Fredsøe) of the proposed fit is below 4%. The corresponding error for the parameterization of u_{*wc} is smaller than 10%.

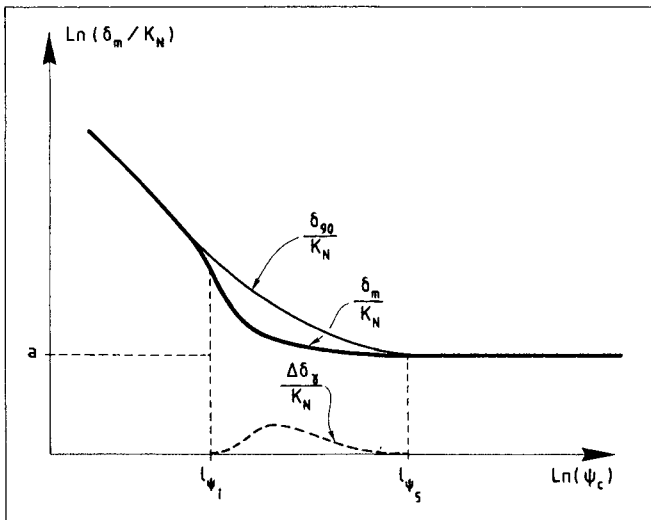


Fig. 3: δ_m parameterization.

5. Closure Submodels

Closure submodels have been obtained from state of art formulations, the main emphasis of this paper being on the numerical model for \vec{u} . The shear stress at z_{tr} can be modeled following (De Vriend and Stive 1987) and (Svendsen 1984/85), with an equation which includes the effects of the carrying wave, the roller and a possible free surface boundary layer. Alternatively it can also be modeled using the (Deigaard and Fredsøe 1989) and (Deigaard et al. 1991) equations adapted to a 3D case. These equations, including contributions from the wave motion, the roller and the set up, have been assumed to be valid, in the direction of the wave number vector \vec{K} , for a horizontally varying problem.

The closure submodel for ν_V is, at present:

$$\nu_V(z, x) = \frac{\kappa u_{*c}}{z_{tr}} z (z_{tr} - z) + M \left(\frac{D}{\rho}\right)^{1/3} \frac{z^2}{z_{tr}} \tag{20}$$

With D the mean rate of wave energy dissipation per unit area and M a parameter of order 10^{-2} . The first term represents the current-induced eddy viscosity and is similar to the one proposed by Coffey and Nielsen (1984). Very near the bottom this term varies approximately in a linear manner with z , which is consistent with the linear variation assumed by our BBL model.

The second term (after vertical integration) is similar to previous proposals for the breaking induced eddy viscosity (e.g. De Vriend and Stive 1987, Battjes 1983). The total ν_V is parabolic with z , which is in accordance with the latest experimental information (see figure 4).

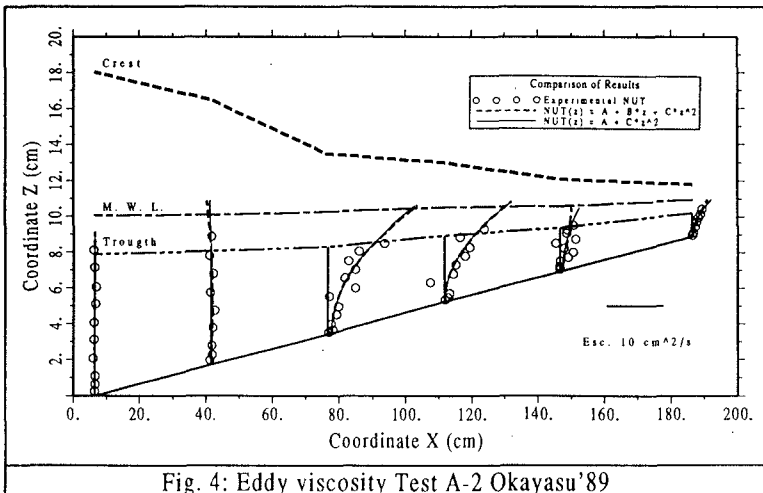


Fig. 4: Eddy viscosity Test A-2 Okayasu '89

The resulting expression may be formally written as:

$$\nu_V(\xi) = a + c\xi^2 \tag{21}$$

in which ξ is a normalized vertical coordinate ranging from 0 (at the actual bottom) to 1 (at the z_{tr} level).

6. Calibration

At this stage the model is being calibrated for a 2DV flume case, using a very complete set of data from Okayasu (1989) experiments. Figures 5 and 6 depict preliminary computed undertow profiles (corresponding to case A2 of Okayasu 1989 tests). These results have been obtained using measured data instead of external closure submodels, the main aim being the calibration of the numerical solution technique for \tilde{u} . The list of measured data used in the simulation is the following: wave height, wave period, water depth, trough level, mean velocity and its horizontal gradient, vertical velocity at z_{tr} , shear stress at z_{tr} and eddy viscosity values at z_{tr} and z_b . The orbital velocity and amplitude near the bottom have been estimated using linear long wave theory.

The next step of the calibration process corresponds to cases with oblique wave incidence for the following geometries: i) cylindrical beach, ii) semicircular bay and iii) longshore-uniform beach with a river mouth. All these test cases have been proposed within the G8M-MAST II Project.

Finally, it is convenient to remark the importance of continuing theoretical and experimental research to improve and "tune" the different closure submodels. The final solution appears to be strongly dependent on these closure relationships.

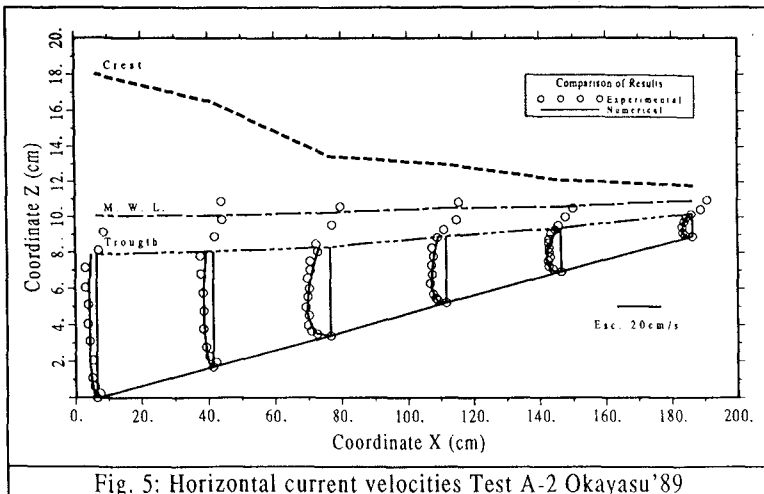


Fig. 5: Horizontal current velocities Test A-2 Okayasu '89

Table 1: Test case A2

The list of measured data used in the simulation of case A2 is:

type of breaking: plunging

wave height (H) : 7.36 cm , wave period (T) : 1.5 s

water depth (h) : 3.66 cm

trough level (z_{tr}) : 2.40 cm

mean velocity (\bar{u}) : 4.86 cm/s

horizontal gradient of \bar{u} ($\frac{\partial \bar{u}}{\partial z}$) : 0.014 1/s

vertical velocity at z_{tr} ($w(z_{tr})$) : 0.1 cm/s

vertical distribution of $w(z)$

eddy viscosity at z_{tr} ($\nu_t(z_{tr})$) : 3.0 cm**2/s

eddy viscosity at z_b ($\nu_t(z_b)$) : 1.0 cm**2/s

bottom roughness (estimated) (K_N) : 1.0 mm.

orbital amplitude (a) or max. free stream velocity (Um) (estimated by linear long wave theory) : 24.6 cm/s

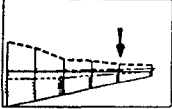
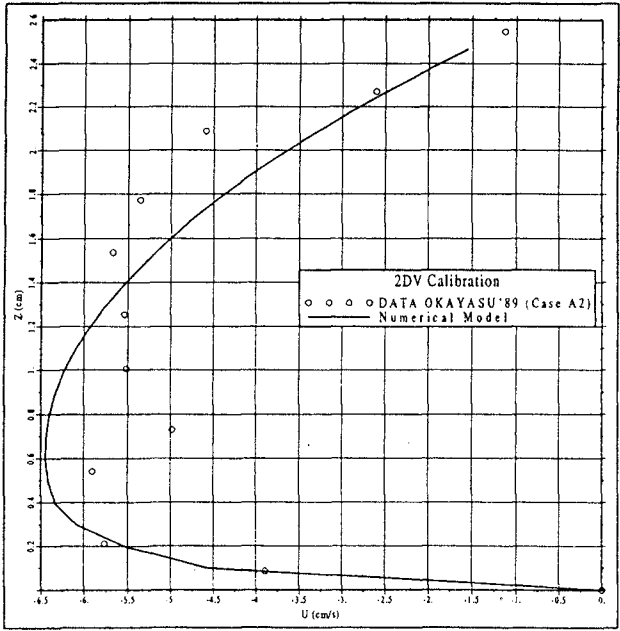



Fig. 6: Measured and computed velocities.

7. Discussion and Future Work

7.1 Discussion: An economic strategy to combine a 2DH Surf Zone circulation code with a 1DV "profile extraction" model has been established. The use of the current (in the presence of waves) friction velocity, u_{*c} , as a degree of freedom to solve the apparent over-statement of the problem works well for a ν_V corrected by breaking effects at the top of the bottom boundary layer.

The ν_V values given by the bottom boundary layer model are well below the experimental values of ν_V inside the surf zone. This explains the relatively strong curvature of the \hat{u} profile right above the bottom boundary layer, which is not very consistent with the experimental data. This means that the ν_V increment at z_b must be larger than the increase given by the bottom boundary layer relationship ($\nu_V(z_b) = \kappa u_{*c} z_b$). This increment is given in the model by the addition the breaking-induced of ν_V .

From the standpoint of the numerical solution, the \vec{u} equation becomes ill-conditioned for very small values of ν_V . This is because there is a singularity at z_b when $\nu_V(z_b) = 0$. At this singularity the coefficients of the series expansion become inordinately large. Similar problems also appear with large ν_V values near trough level.

The number of terms required in the power series development for $\hat{u}(z)$, inside the surf zone, depends on the type of z -dependence assumed for ν_V . The number of terms used is determined by checking that the zero vertical-average condition for \vec{u} (mass conservation) is accurately satisfied.

The undertow profiles, considered to be more demanding from the standpoint of this model validation, were selected as the first case for calibration. For the \hat{v} equation (basically the longshore current) the double-logarithm hypothesis at z_b of the BBL model is expected to hold much more easily (the changes in vertical curvature of $\hat{v}(z)$ are much smaller).

7.2 Future work: With respect to future work there are three main tasks already under way:

- To check the theoretical compatibility between the expressions for $\langle \vec{\tau}_{ir} \rangle$ and the corresponding equations for the wave-driving terms, \vec{W}_i .
- To analyze the model sensitivity to the ν_V value at z_b and to obtain $\nu_V(z)$ closure sub-models which provide a better fit to the observed $\vec{u}(z)$.
- To test and improve all external closure sub-models.

The next step is, obviously, to run the model for a true 3D problem, to prove its quasi-3D capabilities. This in spite of the lack of reliable 3D data inside the surf zone.

8. Acknowledgements

This work was undertaken as part of the MAST-G6 Coastal Morphodynamics research programme. It was funded jointly by the Programa de Clima Marítimo (PCM-MOPT), Ministerio de E. y C. of Spain and by the Commission of the European Communities D.G.XIII under contract no. MAST-0035-C. Thanks are due to all research staff of LIM-UPC, particularly to Mr. F. Rivero, Mr. M. Coussirat and Mr. J. Flores. The experimental information was kindly facilitated by Dr. A. Okayasu.

9. References

- Battjes, J. (1983) "Surf zone turbulence". Proc. 20th IAHR Cong., Moscow.
- Coffey, F.C. and Nielsen, P. (1984) "Aspects of Wave Current Boundary Layer Flows". Proc. I.C.C.E., ASCE, pp 2232-2245.
- Deigaard, R. and Fredsøe, J. (1989) "Shear stress distribution in dissipative water waves". Coastal Engineering, 13, pp. 357-378.
- Deigaard, R.; Justensen, P. and Fredsøe, J. (1991) "Modelling of Undertow by one equation turbulence model", Coastal Engineering, 15, N° 5-6.
- De Vriend, H. and Stive, M.J.F. (1987) "Quasi-3D modelling of nearshore currents". Coastal Engineering, 11, pp 565-601.
- Dingemans, M.; Radder, A. and De Vriend H. (1987) "Computations of the driving forces of wave-induced currents". Coastal Engineering, 11, pp 539-563.
- Fredsøe, J. (1984) "The turbulent boundary layer in Wave-Current Motion", J.H.E, ASCE, Vol 110, N° 8, pp 1103-1120.
- Okayasu, A. (1989) "Characteristics of turbulence structure and undertow in the surf zone", Ph.D. thesis, University of Tokio, Japan.
- Rivero, F. and Sánchez-Arcilla, A. (1992) "Propagation of linear water waves over slowly varying depth and currents". LIM-UPC, Internal report, Universidad Politécnica de Cataluña, Barcelona.
- Sánchez-Arcilla, A.; Collado, F.; Lemos, C. and Rivero, F. (1990) "Another quasi-3D model for surf-zone Flows", ICCE, ASCE, Delft, pp. 316-329.
- Sánchez-Arcilla, A.; Collado, F. and Rodriguez A. (1991) "Nearshore model for Q-3D Nearshore Circulation". Proc. Mid-Term Workshop Coastal Morphodynamics, Edimburg, G6M-MAST, 2.16.
- Simons, R.; Kyriacou, A.; Soulsby, R. and Davies, A. (1988) "Predicting the nearbed turbulent flow in waves and currents". Proc. IAHR Symp., Copenhagen, pp 33-47.
- Svendsen, I.A. (1984) "Mass Flux and Undertow in a Surf-Zone". Coastal Engineering 8, pgs. 299-307.
- Svendsen, I.A. (1985) "On the formulation of the cross shore Wave-current problem". European workshop on Coastal Zones, Athens, pp 1.1-1.9.
- Yoo, D. (1986) "Mathematical modelling of waves-currents interacted flow in shallow waters". Ph.D. Thesis, University of Manchester, U.K.
- Yoo, D. and O'Connor (1988) "Diffraction of waves in caustic". JWW, ASCE, Vol 114, No. 6, pp 715-731.